Enzyme-Controlled Self-Assembly and Transformation of Nanostructures in a Tetramethylbenzidine/Horseradish Peroxidase/H_2O_2 System

Lizeng Gao,[†] Jiamin Wu,[†] and Di Gao*

Department of Chemical and Petroleum Engineering, University of Pittsburgh, Pittsburgh, Pennsylvania 15261, United States. [†]These authors contributed equally to this work.

ABSTRACT Enzyme-assisted bottom-up nanofabrication has attracted considerable attention because it provides an ideal strategy for fabricating and tailoring well-defined nanostructures with desired properties under physiological reaction conditions. Here, we report self-assembly and transformation of nanostructures controlled by enzymatic kinetics in a system consisting of horseradish peroxidase (HRP), hydrogen peroxide (H_2O_2), and 3,3′,5,5′-tetramethylbenzidine (TMB). In this system, several TMB derivatives, produced in the presence of the enzyme HRP at different concentrations, assemble into nanoscale structures in a variety of morphologies and colors. Significantly, the assembly process is reversible, resulting in transformation of the synthesized nanostructures from one morphology into another through disassembly and reassembly processes under physiological conditions. The capability of synthesizing and controlling these "nano-transformers" through tuning enzymatic kinetics creates new opportunities for synthesis of smart materials and biomimetic nanofabrication.

KEYWORDS: nanostructures · self-assembly · transformation · enzyme kinetics

Enzyme-controlled self-assembly and disassembly systems are omnipresent in vital biological processes. The high degree of sophistication and miniaturization of such systems has inspired scientists to combine enzymatic control and molecular assembly as a powerful new approach to synthesizing novel nanomaterials.[1−4] Since its emergence, enzyme-controlled nanosynthesis has attracted considerable attention for complex macromolecular assemblies with controlled shapes, selected affinities, and rich structural combinations that offer diverse functions in biomimetic applications.[2,5−14] A significant advantage of the enzyme-assisted nanosynthesis approach, compared to alternative routes of chemical preparation, is that the synthesis may be carried out with promising efficiency and high selectivity under physiological reaction conditions without the use of toxic reagents or organic solvents. To date, most studies have focused on synthesis of nanostructures in one specific morphology, but very few reports discuss assembly of nanostructures in distinctively different morphologies and, particularly, transformation of nanostructures from one morphology into another in one reaction system.

Here, we report self-assembly of nanostructures in diverse morphologies and colors in a reaction system consisting of horseradish peroxidase (HRP), hydrogen peroxide (H_2O_2), and 3,3′,5,5′-tetramethylbenzidine (TMB). In this system, several TMB derivatives, produced in the presence of the enzyme HRP at different concentrations, assemble into structures in distinctively different morphologies, including straight nanobelts, curved nanobelts, and nanospheres in diverse colors, controlled by the enzymatic kinetics. Significantly, by altering the enzyme concentration in the system, the assembly process may be reversed and the synthesized nanostructures become "nano-transformers", capable of transforming into different morphologies through disassembly and reassembly processes under physiological conditions.

RESULTS AND DISCUSSION

TMB is the most common chromogenic substrate for HRP (EC 1.11.1.7), typically used as a benign and noncarcinogenic color reagent in enzyme-linked immunosorbent assay (ELISA). The oxidation of TMB by HRP/H_2O_2 in acetate buffer (pH 4.0) produces a blue color (Figure 1a), with major absorbance peaks at 370 and 652 nm. The blue color changes to yellow with maximum absorbance at 450 nm when the reaction is stopped by adding sulfuric acid (Figure 1b). In a typical ELISA experiment, the color is developed quickly in 10−20 min, which is sufficient for analysis purposes.[15,16] However,

* Address correspondence to gaod@pitt.edu.

Received for review June 22, 2011 and accepted July 15, 2011.

Published online July 15, 2011
10.1021/nn2023107

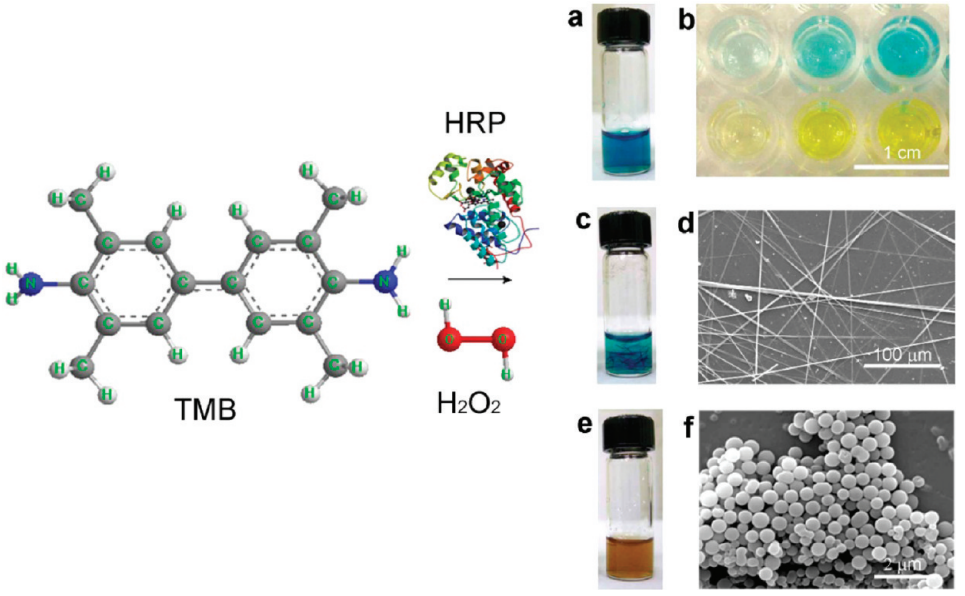

Figure 1. Color reaction and formation of nanostructures in the HRP/H_2O_2/TMB system. (a) Oxidation of TMB by HRP/H_2O_2 in acetate buffer (pH 4.0) produces a blue color. (b) Blue color (top row) changes to yellow (bottom row) upon addition of sulfuric acid for typical ELISA analysis. (c) Blue nanobelts are formed after allowing the blue solution to react for 24 h at room temperature. (d) SEM image of nanobelts. (e) Upon mixing additional HRP to the blue mixture of aqueous solution and nanobelts, the color of the system turned brown, accompanied by precipitation of uniform nanoparticles. (f) SEM image of nanoparticles.

when allowing the blue solution to react for 24 h at room temperature without stopping it with sulfuric acid, to our surprise, a large quantity of nanobelts, with lengths up to 1 mm, precipitated out of the solution (Figure 1c,d). More interestingly, upon mixing additional HRP to this blue mixture of aqueous solution and nanobelts, the color of the system turned brown (Figure 1e), accompanied by precipitation of uniform nanoparticles (Figure 1f). These phenomena indicate that this reaction system enables synthesis of nanostructures in completely different morphologies and transformation of these nanostructures from one morphology to another under control of enzymatic kinetics, which intrigue us to study the role that enzymatic kinetics plays in these processes.

First, we investigated the influence of enzyme concentration on the formation of nanostructures while keeping the concentrations of H_2O_2 (8.1 mM) and TMB (1.38 mM) constant (details of the reaction system are described in Methods). When a low concentration of HRP (12.5 nM) was used in the reaction system, long and straight nanobelts in a blue color were formed at a slow rate, and the nanobelts stopped growing after about 24 h, with a final dimension of 100 nm to 1 μm in width, 50 to 500 nm in thickness, and up to 1 mm in length (Figure 2a). When the HRP concentration was increased to 25 nM, both nanoparticles (800−1200 nm in diameter) and nanobelts were observed (Figure 2b) and both stopped growth after about 24 h. When the HRP concentration was increased to 50 nM, only nanoparticles were observed (Figure 2c), which were smaller (500−800 nm in diameter) compared to the nanoparticles synthesized when 25 nM HRP was used. The

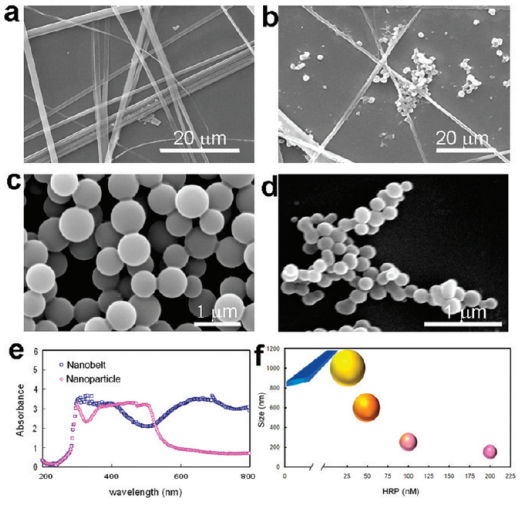

Figure 2. Nanostructures in diverse morphologies and colors synthesized by using varied concentrations of HRP. (a) Nanobelts formed when the HRP concentration was 12.5 nM. (b) Nanobelts and nanoparticles formed when the HRP concentration was 25 nM. (c) Nanoparticles formed when the HRP concentration was 50 nM. (d) Nanoparticles formed when the HRP concentration was 200 nM. (e) Representative absorbance spectra of the reaction mixtures in which nanobelts and nanoparticles were synthesized when the HRP concentrations were 12.5 and 50 nM, respectively. (f) Schematic relationship between the HRP concentration and the morphology and color of nanostructures synthesized in this reaction system.

reaction rate was apparently faster, and the nanoparticles stopped their growth after about 5 h. Beyond 50 nM, higher concentrations of HRP resulted in faster reaction rates and the formation of even smaller nanoparticles. For example, nanoparticles stopped growth in 2 h with a final diameter of 200−300 nm when 100 nM

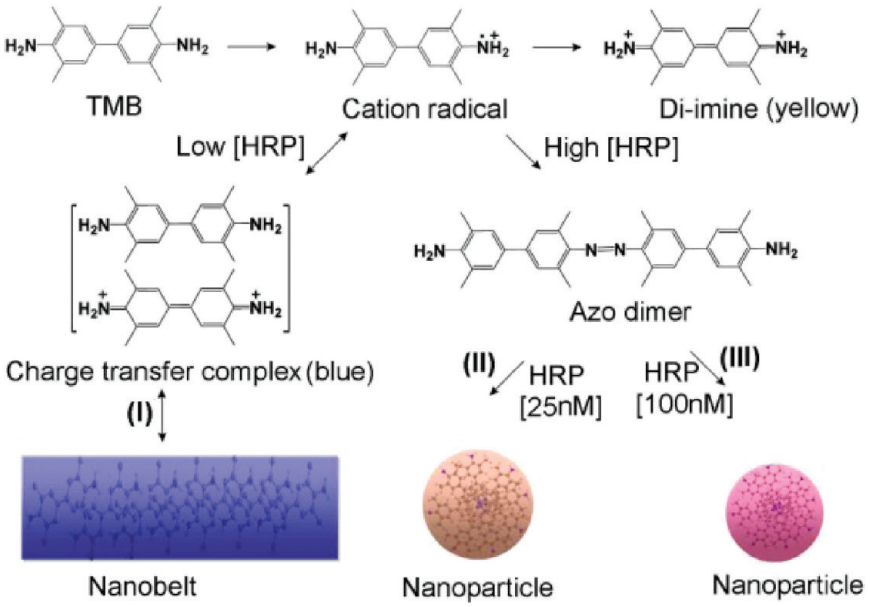

Scheme 1. Route for the enzyme-controlled assembly and transformation of nanostructures in diverse morphologies and colors in the HRP/H_2O_2/TMB system.

HRP was used, and nanoparticles stopped growth in 1 h with a final diameter of 150−200 nm (Figure 2d) when 200 nM HRP was used. Different HRP concentrations also resulted in different colors displayed by the reaction mixtures. Figure 2e shows representative absorbance spectra of two reaction mixtures with distinctively different colors (blue and brown) in which nanobelts and nanoparticles were synthesized by using HRP concentrations of 12.5 and 50 nM, respectively. In addition to the different colors displayed by the reaction mixture, the as-prepared nanoparticles also displayed different colors varying from light yellow to red, as schematically represented in Figure 2f, after they were separated and redispersed in deionized (DI) water. The absorbance spectra of two representative yellow and red nanoparticle dispersions are shown in Supporting Information Figure S1.

A plausible mechanism for synthesis of nanostructures in such diverse morphologies and colors is schematically presented in Scheme 1, based on our experimental results and previous studies of the HRP/H_2O_2/TMB system. With the presence of HRP and H_2O_2, there may be several TMB derivatives in the reaction system, including intermediates (*e.g.*, cationic free radical, charge-transfer complex, and di-imine) and end product (azo dimer).[15,17] The charge-transfer complex exhibits a blue color, with absorbance peaks at 652 and 370 nm, while the di-imine displays a yellow color, with an absorbance peak at 450 nm. In a traditional ELISA assay, a blue signal produced by the TMB with the presence of trace amount of HRP comes from the charge-transfer complex, consisting of a cation free radical and TMB. This charge-transfer complex tends to assemble into belt-shape nanostructures in solution through stacking of its aromatic molecular structure (Scheme 1I).[18,19] Raman spectra of the nanobelts show characteristic bands that are associated with the charge-transfer complex (Supporting Information Figure S2I), implying that the nanobelts are assembled from this blue complex. When high concentrations (more than 25 nM in our experiment) of HRP are used, the excessive enzyme drives the reaction toward production of the end product, azo dimer, through dimerization of the cation free radical. As a highly hydrophobic molecule, the azo dimer has a much lower solubility than TMB in aqueous solutions and aggregates quickly into nanoparticles (Scheme 1II,III). This reaction mechanism is supported by the Raman spectrum of the synthesized nanoparticles (Supporting Information Figure S2II), which implies that −N═N− coupling occurs during the dimerization of the cation free radical and the formation of nanoparticles. The proposed two different routes through which the nanobelts and the nanoparticles are synthesized, respectively, are also consistent with the absorbance spectra of the two reaction mixtures (Figure 2e), where the mixture for synthesizing the nanobelts shows a clear absorbance peak at around 652 nm that the mixture for synthesizing the nanoparticles does not possess, corresponding to the absorbance of the charge-transfer complex.

Formation of the nanoparticles starts with aggregation of the hydrophobic azo dimers, which is likely to take place near the HRP where the azo dimer is produced and present in a locally high concentration. Therefore, for a given TMB concentration, higher concentrations of HRP may result in more nucleation centers for the formation of the nanoparticles, which lead to formation of more particles at more rapid rates but with smaller sizes. The absorbance spectra of all the dispersions of the nanoparticles, separated from the reaction mixture

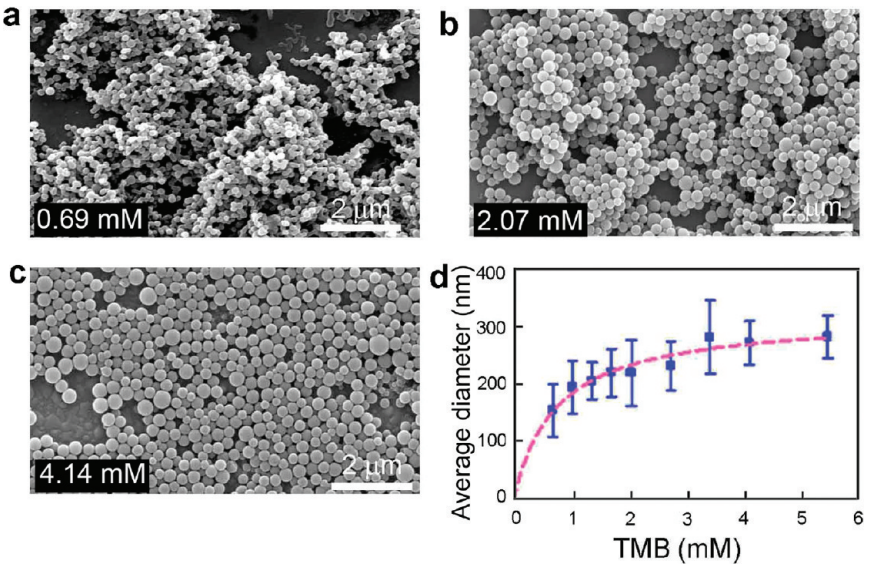

Figure 3. Effects of TMB concentrations on the nanostructure assembly process. (a–c) SEM images of nanoparticles synthesized by using 0.69, 2.07, and 4.14 mM TMB, respectively. (d) Average diameter of nanoparticles as a function of TMB concentration. The dotted line is added to guide the eye.

and dispersed in DI water, have a peak at approximately 310 nm (Supporting Information Figure S1), which may be attributed to the π–π^* transition of the benzenoid rings and lead to a reddish color for the dispersion when visually inspected. The yellowish color of the nanoparticles when the HRP concentration is between 25 and 100 nM may be due to incorporation of di-imine into the nanoparticles. The di-imine has an absorbance peak at 470 nm, which is consistent with the shoulder around 470 nm shown in the absorbance spectrum of the yellow nanoparticles (Supporting Information Figure S1). As the HRP concentration increases, the nanoparticles grow more rapidly and less di-imine is incorporated into the nanoparticles; therefore, the color of the nanoparticles changes gradually from yellow to red.

Next, we investigated the effect of the substrate concentration on the nanostructure assembling process. HRP-mediated catalysis follows a ping-pong mechanism in which the enzyme first reacts with H_2O_2 to form an enzyme-oxygen free radical and then the free radical reacts with TMB.[20,21] Therefore, concentrations of both TMB and H_2O_2 will affect the reaction kinetics. We first examined the effect of TMB concentration by varying it from 0.69 to 5.72 mM while keeping the concentrations of H_2O_2 (8.1 mM) and HRP (100 nM) constant. In all of these experiments, nanoparticles were formed, but the growth rate of the nanoparticles varied as a function of the TMB concentration. To correlate the growth rate to the TMB concentration, we stopped the reaction after 30 min and examined the size of the nanoparticles by scanning electron microscopy (SEM). Figure 3a–c presents representative SEM images of the nanoparticles formed at different TMB concentrations, and Figure 3d plots the average diameter of the nanoparticles as a function of the TMB concentration.

We then examined the influence of H_2O_2 concentration on the nanostructure assembling process. Four concentrations of H_2O_2 (4.05, 8.1, 16.2, and 32.4 mM) were examined, while the concentrations of TMB (1.38 mM) and HRP (100 nM) were kept constant. When the concentration of H_2O_2 was low (4.05 mM), the formation of nanobelts dominated the assembling process. Increasing the concentration of H_2O_2 to 8.1 mM led to formation of nanoparticles with an average diameter of about 300 nm. Doubling H_2O_2 concentration to 16.2 mM resulted in formation of larger nanoparticles with an average diameter of about 700 nm. However, when the concentration of H_2O_2 was further increased to 32.4 mM, the diameter of the nanoparticles dropped back to about 400 nm. These results indicate that the effect of H_2O_2 concentration on the nanostructure assembling process is complex. On one hand, H_2O_2 is a reactant and hence higher concentration of H_2O_2 should lead to faster reaction rate; on the other hand, H_2O_2 in high concentrations may become an inhibitor for HRP,[15,22] which slows down the reaction and the nanostructure assembling process.

In addition to the concentrations of HRP, TMB, and H_2O_2, the ionic strength of the reaction solution also affects the morphology of the assembled nanostructures. Such an effect is particularly obvious in the formation of nanobelts at low concentrations of HRP. Figure 4a,b presents typical optical and SEM images of straight nanobelts (300 nm to 1 μm wide, 50 to 500 nm thick, and up to 1 mm long) synthesized with 5 nM HRP, 8.1 mM H_2O_2, and 1.38 mM TMB. When the ionic strength of this reaction solution was increased by introducing 100 mM NaCl to the solution, instead of

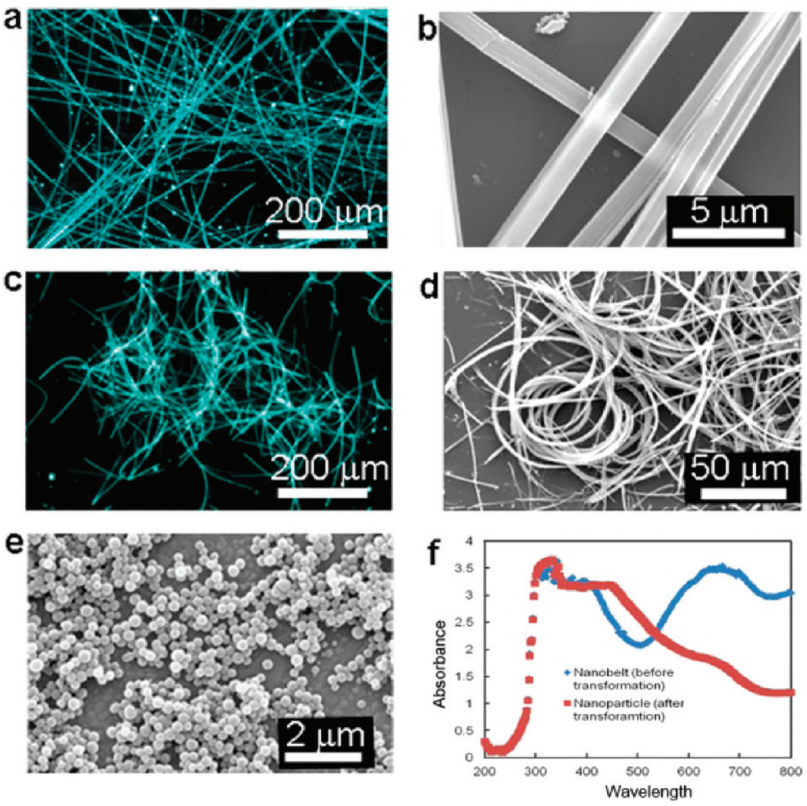

Figure 4. Morphological transformation of nanostructures in the HRP/H_2O_2/TMB system. (a) Optical image of blue straight nanobelts. (b) SEM image of straight nanobelts. (c) Optical image of blue curved nanobelts. (d) SEM image of curved nanobelts. (e) Nanobelts transformed into nanoparticles upon addition of HRP to the reaction mixture. (f) Absorbance spectra of dispersions of nanobelts and nanoparticles taken before and after the morphological transformation, respectively.

forming long and straight belts, much shorter (300–600 μm in length), curved, and flexible nanobelts (Figure 4c,d) were formed. Interestingly, both straight and curved nanobelts were able to completely disassemble and dissolve when they were separated from the reaction mixture and placed in DI water. Furthermore, the two types of belts can transform into each other for unlimited number of cycles upon changing the ionic strength of the solution by adding or removing NaCl. Supporting Information Figure S3 shows optical images and the absorbance spectra taken during the nanobelt disassembly process. The solution of the dissolved curved belts shows the same optical absorbance characteristic as that of the dissolved straight belts, which indicates that the molecular structure of the two types of belts are likely the same charge-transfer complex as shown in Scheme 1. The results imply that assembly of this intermediate complex is reversible (as represented by the two-way arrow for the assembly process I in Scheme 1) and may be affected by small anions, such as chloride, which lead to the formation of curved nanobelts.

Inspired by our capability of triggering the morphological transformation of the nanobelts through altering the ionic strength of the solution, we explored the possibility of triggering more significant morphological changes—from nanobelts to nanospheres—by altering the enzyme HRP concentration in this system. Indeed, upon adding HRP to the reaction mixture in which nanobelts, either straight (Figure 4a,b) or curved (Figure 4c, d), had been formed, the nanobelts gradually dissolved, followed by formation of nanospheres (Figure 4e). A possible route for disassembly of nanobelts and spontaneous formation of nanospheres can be clearly seen in Scheme 1. The nanobelts may dissemble into the charge-transfer complex, which can be further oxidized to the final product of azo dimer through another intermediate TMB derivative, the cation radical, with the presence of high concentrations of HRP. The absorbance spectra (Figure 4f) taken before and after the morphological transformation indicate that the absorbance of nanobelts around 652 nm (characteristic absorbance of the charge-transfer complex) is significantly reduced after they transform into nanoparticles, which supports the proposed route for the morphological transformation.

In conclusion, we have demonstrated that, through controlling the enzymatic reaction kinetics, a variety of nanostructures in diverse morphologies and colors may be synthesized in one reaction system consisting of HRP, TMB, and H_2O_2. The effects of the concentrations of HRP, TMB, and H_2O_2, as well as the ionic strength of the reaction solution on the morphology and color of the assembled nanostructures have been examined. It

appears that the concentration of the enzyme (HRP) plays a more significant role than the concentrations of TMB and H_2O_2 in directing the assembly process and determining the structure of the final product. The importance of enzyme concentration in this reaction system can be employed to trigger spontaneous morphological transformation of the assembled nanostructures by simply controlling the enzyme concentration in the system. In particular, straight and curved nanobelts may be reversibly assembled and disassembled multiple cycles in a physiological environment, and both can transform into nanospheres upon adding enzymes to the aqueous mixture. Such materials may find applications in smart circuitry and bioresponsive devices. The capability of synthesizing and controlling these "nano-transformers" through tuning enzymatic kinetics under physiological conditions may also create new opportunities for synthesis of smart materials and biomimetic nanofabrication.

METHODS

Synthesis of Nanobelts and Nanoparticles. Nanobelts and nanoparticles were synthesized in a HRP/H_2O_2/TMB system. Typically, nanobelts were formed after 24 h of reaction at room temperature in 500 μL of 100 mM NaAc (pH 4.0) solution containing H_2O_2 (8.1 mM), TMB (1.38 mM, Sigma-Aldrich), and a low concentration of HRP (<25 nM, Sigma-Aldrich). Nanoparticles were prepared *via* a 2 h reaction at room temperature in 500 μL of 100 mM NaAc (pH 4.0) solution containing H_2O_2 (16.2 mM), TMB (1.38 mM), and high concentration of HRP (>50 nM). To investigate the effect of enzyme concentration on nanostructures formation, different concentrations (12.5, 25, 50, 100, and 200 nM) of HRP were mixed with H_2O_2 (8.1 mM) and TMB (1.38 mM) in 500 μL of 100 mM NaAc (pH 4.0) at room temperature. To investigate the effect of TMB concentration on nanostructure formation, the TMB concentration was varied from 0.69 to 5.72 mM, and TMB was mixed with HRP (100 nM) and H_2O_2 (8.1 mM) in 500 μL of 100 mM NaAc (pH 4.0) at room temperature. The reaction was stopped after 30 min to examine the synthesized nanostructures. To investigate the effect of H_2O_2 concentration on nanostructure formation, H_2O_2 in four concentrations (4.05, 8.1, 16.2, and 32.4 mM) was mixed with TMB (1.38 mM) and HRP (100 nM) in 500 μL of 200 mM NaAc (pH 4.0) at room temperature. The nanobelts were examined after 24 h of reaction, and the nanoparticles were examined after 2 h of reaction.

Reversible Transformation between Straight and Curved Nanobelts. The straight nanobelts were formed after 24 h of reaction in a mixture of HRP (5 nM), H_2O_2 (8.1 mM), and TMB (1.38 mM) in 500 μL of 100 mM NaAc (pH 4.0) at room temperature. The curved nanobelts were formed after 24 h of reaction in a mixture of HRP (5 nM), H_2O_2 (8.1 mM), TMB (1.38 mM), and NaCl (100 mM) in 500 μL of 100 mM NaAc (pH 4.0) at room temperature. Disassembly of straight and curved nanobelts was observed by separating the nanobelts from the reaction mixture by centrifugation and redispersing the nanobelts in deionized water. Transformation of straight nanobelts to curved nanobelts was observed by adding NaCl (100 mM) to the reaction mixture. Transformation of curved nanobelts to straight nanobelts was observed by separating the curved nanobelts from the reaction mixture and redispersing the nanobelts in a mixture of HRP (5 nM), H_2O_2 (8.1 mM), and TMB (0.138 mM) in 500 μL of 100 mM NaAc (pH 4.0) at room temperature.

Transformation of Nanobelts into Nanoparticles. In a typical reaction system with a low concentration of HRP (*e.g.*, 12.5 nM), nanobelts were first formed after 24 h of reaction at room temperature. Then, appropriate amount of HRP was added to the system, so the final HRP concentration was between 50 and 100 nM. The blue mixture with the nanobelts gradually turned brown. Visible nanoparticle precipitates were observed after 1−2 h. The nanoparticles were collected after 3 h for further characterization.

Characterization. The as-prepared nanobelts and nanoparticles were characterized by optical microscopy, UV−vis spectrometry (Ocean Optics Inc.), and scanning electron microscopy (SEM, Philips XL-30, 15 kV).

Acknowledgment. We thank the Nanoscale Fabrication and Characterization Facility (NFCF) of the University of Pittsburgh for use of the electron microscopy facility.

Supporting Information Available: Representative absorbance spectra of TMB nanoparticle dispersions, Raman analysis of TMB nanobelts and nanoparticles, color change accompanying the disassembly of straight nanobelts in water. This material is available free of charge *via* the Internet at http://pubs.acs.org.

REFERENCES AND NOTES

1. Sanchez, C.; Arribart, H.; Guille, M. M. Biomimetism and Bioinspiration as Tools for the Design of Innovative Materials and Systems. *Nat. Mater.* **2005**, *4*, 277–288.
2. Williams, R. J.; Smith, A. M.; Collins, R.; Hodson, N.; Das, A. K.; Ulijn, R. V. Enzyme-Assisted Self-Assembly under Thermodynamic Control. *Nat. Nanotechnol.* **2009**, *4*, 249–254.
3. Sarikaya, M.; Tamerler, C.; Jen, A. K.; Schulten, K.; Baneyx, F. Molecular Biomimetics: Nanotechnology through Biology. *Nat. Mater.* **2003**, *2*, 577–585.
4. Nanda1, V.; Koder, R. L. Designing Artificial Enzymes by Intuition and Computation. *Nat. Chem.* **2010**, *2*, 15–24.
5. Willner, I.; Baron, R.; Willner, B. Growing Metal Nanoparticles by Enzymes. *Adv. Mater.* **2006**, *18*, 1109–1120.
6. Liu, W.; Cholli, A. L.; Nagarajan, R.; Kumar, J.; Tripathy, S.; Bruno, F. F.; Samuelson, L. The Role of Template in the Enzymatic Synthesis of Conducting Polyaniline. *J. Am. Chem. Soc.* **1999**, *121*, 11345–11355.
7. Ma, Y.; Zhang, J.; Zhang, G.; He, H. Polyaniline Nanowires on Si Surfaces Fabricated with DNA Templates. *J. Am. Chem. Soc.* **2004**, *126*, 7097–7101.
8. Nickels, P.; Dittmer, W. U.; Beyer, S.; Kotthaus, J. P.; Simmel, F. C. Polyaniline Nanowire Synthesis Templated by DNA. *Nanotechnology* **2004**, *15*, 1524–1529.
9. Luckarift, H. R.; Dickerson, M. B.; Sandhage, K. H.; Spain, J. C. Rapid, Room-Temperature Synthesis of Antibacterial Bionanocomposites of Lysozyme with Amorphous Silica or Titania. *Small* **2006**, *2*, 640–643.
10. Eby, D. M.; Schaeublin, N. M.; Farrington, K. E.; Hussain, S. M.; Johnson, G. R. Lysozyme Catalyzes the Formation of Antimicrobial Silvernanoparticles. *ACS Nano* **2009**, *3*, 984–994.
11. Yang, Z. M.; Gu, H. W.; Fu, D. G.; Gao, P.; Lam, J. K.; Xu, B. Enzymatic Formation of Supramolecular Hydrogels. *Adv. Mater.* **2004**, *16*, 1440–1444.
12. Hu, B. −H.; Messersmith, P. B. Rational Design of Transglutaminase Substrate Peptides for Rapid Enzymatic Formation of Hydrogels. *J. Am. Chem. Soc.* **2003**, *125*, 14298–14299.
13. Um, S. H.; Lee, J. B.; Park, N.; Kwon, S. Y.; Umbach, C. C.; Luo, D. Enzyme-Catalysed Assembly of DNA Hydrogel. *Nat. Mater.* **2006**, *5*, 797–801.
14. Hirst, A. R.; Roy, S.; Arora, M.; Das, A. K.; Hodson, N.; Murray, P.; Marshall, S.; Javid, N.; Sefcik, J.; Boekhoven, J.; *et al.* Biocatalytic Induction of Supramolecular Order. *Nat. Chem.* **2010**, *2*, 1089–1094.
15. Josephy, P. D.; Eling, T.; Mason, R. P. The Horseradish Peroxidase-Catalyzed Oxidation of 3,5,3′,5′-Tetramethylbenzidine. *J. Biol. Chem.* **1982**, *257*, 3669–3675.
16. Burns, R. *Immunochemical protocols*, 3rd ed.; Humana Press Inc.: Totowa, NJ, 2005; pp 208−211.

17. Josephy, P. D.; Mason, R. P.; Eling, T. Cooxidation of the Clinical Reagent 3,5,3′5′-Tetramethylbenzidine by Prostaglandin Synthase. *Cancer Res.* **1982**, *42*, 2567–2570.
18. Yang, J.; Wang, H.; Zhang, H. One-Pot Synthesis of Silver Nanoplates and Charge-Transfer Complex Nanofibers. *J. Phys. Chem. C* **2008**, *112*, 13065–3069.
19. Sun, X.; Dong, S.; Wang, E. Formation of *o*-Phenylenediamine Oligomers and Their Self-Assembly into One-Dimensional Structures in Aqueous Medium. *Macromol. Rapid Commun.* **2005**, *26*, 1504–1508.
20. Gajhede, M.; Schuller, D. J.; Henriksen, A.; Smith, A. T.; Poulos, T. L. Crystal Structure of Horseradish Peroxidase C at 2.15 Å Resolution. *Nat. Struct. Biol.* **1997**, *4*, 1032–1038.
21. Gao, L. Z.; Zhuang, J.; Nie, L.; Zhang, J. B.; Zhang, Y.; Gu, N.; Wang, T. H.; Feng, J.; Yang, D. L.; Perrett, S.; *et al.* Intrinsic Peroxidase-like Activity of Ferromagnetic Nanoparticles. *Nat. Nanotechnol.* **2007**, *2*, 577–583.
22. Baynton, K. J.; Bewtra, J. K.; Biswas, N.; Taylor, K. E. Inactivation of Horseradish Peroxidase by Phenol and Hydrogen Peroxide: A Kinetic Investigation. *Biochim. Biophys. Acta* **1994**, *1206*, 272–278.